Influence of surface coverage on the formation of 4,4'-bipyridinium (viologen) single molecular junctions

Henrry M. Osorio,[a,b,f] Santiago Martín,[a,c*] David C. Milan,[d] Alejandro González-Orive,[b] Josef B. G. Gluyas,[e] Simon J. Higgins,[d] Paul J. Low,[e*] Richard J. Nichols,[d*] and Pilar Cea[a,b*]

[a] Departamento de Química Física, Facultad de Ciencias, Universidad de Zaragoza, 50009, Spain.

[b] Instituto de Nanociencia de Aragón (INA), Fundación INA, and Laboratorio de Microscopias Avanzadas (LMA) C/ Mariano Esquilor s/n Campus Rio Ebro, 50018, Zaragoza, Spain.

[c] Instituto de Ciencia de Materiales de Aragón (ICMA), Universidad de Zaragoza-CSIC, 50009 Zaragoza, Spain.

[d] Department of Chemistry, University of Liverpool, Crown Street, Liverpool, L69 7ZD, United Kingdom.

[e] School of Molecular Science, University of Western Australia, 35 Stirling Highway, Crawley, Perth, 6009, Australia.

[f] Departamento de Física, Escuela Politécnica Nacional, Av. Ladrón de Guevara, E11-253, 170525 Quito, Ecuador.

1

Abstract

Single-molecule conductance experiments using the STM-based $I(s)$ method and samples of N,N'-di(4-(trimethylsilylethynyl)benzyl)-4,4'-bipyridinium bis(tetrafluoroborate) ([**1**](BF$_4$)$_2$) prepared on gold substrates with low-surface coverage of [**1**](BF$_4$)$_2$ ($\Gamma = 1.25 \cdot 10^{-11}$ mol·cm^{-2}) give rise to molecular junctions with two distinct conductance values. From the associated break-off distances and comparison experiments with related compounds the higher conductance junctions are attributed to molecular contacts between the molecule and the electrodes via the N,N'-dibenzyl-4,4´-bipyridinium (viologen) moiety and one trimethylsilylethynyl (TMSE) group ($G = (5.4 \pm 0.95) \times 10^{-5}\ G_0$, break-off distance (1.56 ± 0.09) nm). The second, lower conductance junction ($G = (0.84 \pm 0.09) \times 10^{-5}\ G_0$) is consistent with an extended molecular conformation between the substrate and tip contacted through the two TMSE groups giving rise to a break-off distance (1.95 ± 0.12) nm that compares well with the Si...Si distance (2.0 nm) in the extended molecule. Langmuir monolayers of [**1**](BF$_4$)$_2$ formed at the air-water interface can be transferred onto a gold-on-glass substrate by the Langmuir-Blodgett (LB) technique to give well-ordered, compact films with surface coverage $\Gamma = 2.0 \cdot 10^{-10}$ mol·cm^{-2}. Single-molecule conductance experiments using the STM-based $I(s)$ method reveal only the higher conductance junctions ($G = (5.4 \pm 0.95) \times 10^{-5}\ G_0$, break-off distance (1.56 ± 0.09) nm) due to the restricted range of molecular conformations in the tightly packed, well-ordered LB film.

Introduction

Molecular electronics is an emergent technology in which organic, inorganic or organometallic molecules are connected between two (or three) electrodes, and their electrical properties are harnessed to perform some useful function that can translate to enhanced or novel performance in an electronic device.[1] Recent developments in methods of contacting single molecules or portions of monolayer films by electrodes formed from a wide variety of materials, and measuring the electrical characteristics of these 'molecular junctions', have driven significant progress in the area. Nevertheless, many difficult challenges must be overcome before molecular junctions

suitable for developing the science of molecular electronics can be translated to true device structures and considered as a viable technology capable of reaching the market.[2] However, commercial molecular electronics devices are starting to emerge with the innovation of molecular electronic components for audio processing.[3]

Many studies have been undertaken to measure and optimize the electrical characteristics of molecular junctions, with an ultimate goal of establishing design rules for the construction of a molecular electronic device. It is now well-established that charge transfer through molecular junctions is dependent on many different factors, including the structure and conformation of the molecular backbone, the number of molecules in the junction, solvent environment and external electrochemical potential, the electrode material, surface structure and the nature of the electrode-molecule contact.[4-7] The study of single molecule junctions has greatly contributed to the understanding of these parameters, and their influence on charge and heat transport phenomena at the molecular scale.[8-16] Although single molecule measurements may appear to represent the ultimate low coverage phase (i.e. a single molecule), depending on the measurement conditions, such measurements may also be performed on single molecules within a densely packed monolayer phase. In turn, studies of larger area metal–molecular monolayer–metal junctions in which molecular components are assembled into a well-defined, high surface coverage and usually well-characterized monolayer film within the junction play a further crucial role in understanding the effect of intermolecular interactions, such as van der Waals interactions and polarization effects, on the electronic transport properties of the molecular film.[17-20] In addition, whilst single molecule junctions are excellent vehicles through which to study transport phenomena, planar-sandwiched monolayer structures are more closely aligned with practical electronic applications.

Whether assembled from a single-molecule or monolayer-film, the ability to manipulate the electrical response of a molecular junction beyond the simple non-resonant tunneling behavior of many candidate molecular wires is also an area of intense contemporary activity. For example, mechanical compression or elongation of single-molecule junctions has been shown to facilitate the manipulation of the structure of the molecule within the junction and details of how molecules bind to the electrodes, resulting in mechanical gating of the junction.[21, 22] However, despite

establishing that molecular orientation and junction geometry can play a significant role on the electrical response of a junction, it is not yet clear how, or if, the changes in molecular geometry and orientation that can be expected to occur upon increasing surface coverage of molecular components from truly isolated single molecules to more densely packed and ordered films can influence the electrical response of a junction.

The capacity of various *N,N'*-disubstituted-4,4'-bipyridinium, or viologen, derivatives to assemble into well-ordered mono- and multi-layered Langmuir films has been established.[23-25] In these structures, the doubly-charged viologen group is anchored at the aqueous surface and the (typically hydrophobic) *N,N'*-substituents are aligned outwards from the surface of the aqueous sub-phase.[23, 26] These Langmuir films are readily transferred onto hydrophilic substrates by means of the vertical dipping method,[23, 26, 27] preserving the orientation of the viologen units in the Langmuir films in the resulting substrate-supported Langmuir-Blodgett film. The electrochemical properties of these well-ordered films have been characterized but the electrical properties of these films have not yet been studied in detail.

Viologen-based molecular components have also been studied within single molecule junctions, with the reversibility of their redox reactions at modest potentials and the high chemical stability of their various redox states leading to effective molecular junctions featuring hopping mechanisms. This has facilitated electrochemical switching and development of nascent transistor-like devices.[11, 28-30] However, a comparative study of viologen-containing molecules within both single molecule junctions and well-ordered films offers additional challenges and avenues for exploration that have not been explored to date.

In this contribution, single-molecule junctions of the viologen derivative, *N,N'*-di(4-(trimethylsilylethynyl)benzy)-4,4'-bipyridinium as its bis(tetrafluoroborate) salt ([**1**](BF$_4$)$_2$) (Figure 1) have been formed from both dilute solution, leading to low surface coverage, and, on the other hand, well-ordered and tightly-packed monolayer LB films. The surface coverage dependence of the formation of single molecular junctions and the resulting electrical conductance is evaluated. The electrical properties and break-off distances from the single molecule junctions formed from

isolated molecules of [**1**](BF$_4$)$_2$ on the surface and well-ordered films reveal two distinct conductance values. By comparison with junctions formed from the related compounds [**2**](BF$_4$)$_2$ and **3** (Figure 1) these different conductance values can be attributed to different molecular configurations and contacts within the junction: (1) a lower conductance junction formed from electrode contact to the two terminal trimethylsilylethynyl (TMSE) groups with the molecule adopting an extended conformation between the electrodes; and (2) a higher conductance junction arising from a more compact molecular conformation with contact to the electrodes formed between the viologen moiety and one TMSE group. Both types of molecular contact are observed for junctions formed from the isolated molecules, but in the case of the LB film-based junctions, only the more compact, viologen-contacted junction has been observed.
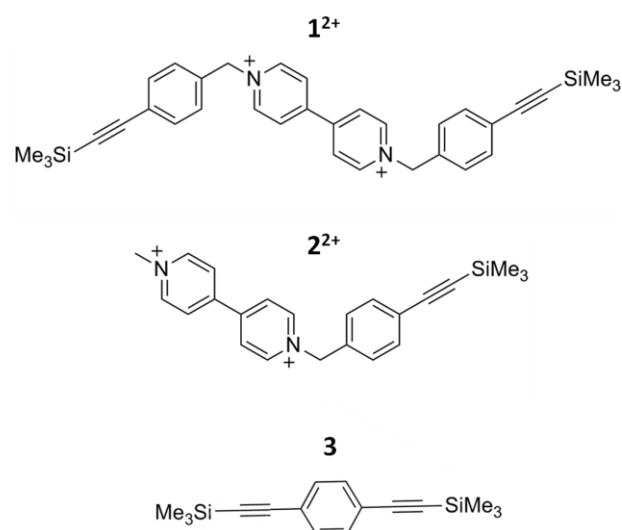

Figure 1. Molecular structures of the compounds used in this study.

Experimental Methods.

Compound [**1**](BF$_4$)$_2$ and **3** were synthesized by the literature methods.[30, 31] Compound [**2**](BF$_4$)$_2$ was prepared by minor variation of the routes described elsewhere.[32]

LB films of [**1**](BF$_4$)$_2$ were prepared using a Nima Teflon trough with dimensions (720×100) mm^2, which was housed in a constant temperature (20 ± 1 °C) clean room. A Wilhelmy paper plate pressure sensor was used to measure the surface pressure (π)

of the monolayers. The subphase was pure water (Millipore Milli-Q, resistivity 18.2 $M\Omega\cdot cm$). A 7.5×10^{-6} M solution of [**1**](BF$_4$)$_2$ in HPLC grade CHCl$_3$:EtOH (3:1) was spread onto the water surface. The spreading solvent was allowed to completely evaporate from the aqueous surface over a period of at least 20 min before compression of the monolayer commenced at a constant sweeping speed of 0.015 nm$^2\cdot$molecule$^{-1}\cdot$min^{-1}. Under these experimental conditions, the isotherms were highly reproducible. The monolayers were deposited by the vertical dipping method onto a gold substrate at a constant surface pressure of 10 mN$\cdot$m^{-1} and a speed of 3 mm$\cdot$min^{-1}.

The STM based $I(s)$ method described in the literature,[11, 33] and in further detail in the Supporting Information, has been used here to obtain conductance values of molecular junctions formed from either a LB film of [**1**](BF$_4$)$_2$ or low coverage phases of compounds [**1**](BF$_4$)$_2$, [**2**](BF$_4$)$_2$ and **3**. The STM-$I(s)$ measurements were performed with flame-annealed Au substrates which feature Au(111) microfacet.[34] Molecular adsorption for the low coverage single-molecule studies was achieved by immersing the gold electrode for 60 s in a 5×10^{-4} M ethanolic solution. This short immersion time and low concentration is excepted to yield low surface coverage (see main text). After adsorption, the sample was rinsed in ethanol and gently blown dry in a stream of nitrogen gas. Gold STM tips were fabricated from 0.25 mm Au wire (99.99%) which was freshly electrochemically etched for each experiment at +2.4 V in a mixture of ethanol (50%) and HCl (50%).

Results and discussions

The low surface coverage deposition of [**1**](BF$_4$)$_2$ on a flame-annealed gold substrate was achieved by placing a gold electrode for just 60 s into a 5×10^{-4} M solution of [**1**](BF$_4$)$_2$ in ethanol. The surface coverage at this time, 60 s, was quantified by measuring the frequency change (Δf) of a quartz crystal resonator for incubation at different times in the adsorption solution until the frequency remained constant (see SI, for further details). Using the Sauerbrey equation,[35] the frequency change was converted to coverage. At an immersion time of 60 s a surface coverage of $1.25\cdot10^{-11}$ mol$\cdot$cm^{-2} was obtained.

A higher surface coverage of [**1**](BF$_4$)$_2$ was obtained by transferring a homogenous monolayer, formed and characterized at the air-water interface, onto a gold substrate to produce a compact LB film. This was achieved by the vertical dipping method with the hydrophilic substrates initially immersed in the water subphase at the optimum surface pressure of 10 mN·m^{-1} (see SI for further details of the LB film fabrication and characterization). At this surface pressure the surface coverage was determined with a quartz crystal microbalance (QCM) by measuring the frequency change (Δf) for a quartz resonator before and after the deposition process. A surface coverage, Γ, of $2.0 \cdot 10^{-10}$ mol·cm^{-2} was then obtained using the Sauerbrey equation (see SI). Therefore, from these two different methods of sample preparation, a surface coverage difference amounting to a factor of 16 between the low and high coverage is obtained, allowing us to study how these two markedly different surface arrangements of **1**$^{2+}$ influence the formation of molecular junctions using an STM probe.

Conductance measurements of molecular junctions formed from either low surface coverage phases ($\Gamma = 1.25 \cdot 10^{-11}$ mol·cm^{-2}) or LB films (high surface coverage, $\Gamma = 2.0 \cdot 10^{-10}$ mol·cm^{-2}) of [**1**](BF$_4$)$_2$ were carried out using a scanning tunneling microscope (STM) and the $I(s)$ method.[11, 33] The $I(s)$ method has been widely used to determine the conductance both of single molecules[14, 36-38] and molecules assembled into monolayers.[39-42] In the $I(s)$ technique, an STM tip is first moved into close proximity of the surface, by adjusting the set-point current (I_0) to high values. However, in contrast to the STM break-junction method direct metallic contact between tip and surface is avoided. The STM feedback loop is then temporarily switched off and the STM tip is rapidly retracted while recording the junction tunneling current. An enhanced junction current results if a molecular bridge forms between the STM tip and substrate. Many such molecular junction formation and cleavage cycles are recorded and statistically analyzed in histograms to obtain the molecular junction conductance. Further details of the measurements are given in the SI.

The $I(s)$ curves obtained at a set-point current of 40 nA from substrates with low surface coverage of [**1**](BF$_4$)$_2$ feature a set of plateaus arising from formation of single-molecule junctions, with a relative high conductance (HC) value at (5.3 ±

$0.85)\times10^{-5}$ G_0 (Figure 2a), with a break-off distance of (1.6 ± 0.11) nm, estimated from the corresponding 2-D histogram (Figure 3a), which is somewhat shorter than the Si...Si distance estimated for the extended molecular conformation (2.0 nm). A detailed analysis closer to the noise level of the current amplifier in the $I(s)$ scans of these conductance-distance traces shows another set of plateaus that are clustered around a low conductance (LC) value of $(8.4 \pm 0.9)\times10^{-6}$ G_0, almost an order of magnitude lower than the HC feature, with a much longer break-off distance of 1.95 ± 0.12 nm (Figure 3c). The plateaus corresponding to the LC feature and the corresponding conductance histogram are illustrated in the insets to Figure 3a.

Some of the sample conductance traces were found to have plateaus corresponding to both conductance values, suggesting that the conduction pathway in the high state (HC) is not only shorter than that in the low state (LC), but that the HC junctions can evolve into the LC junctions as the tip is retracted.
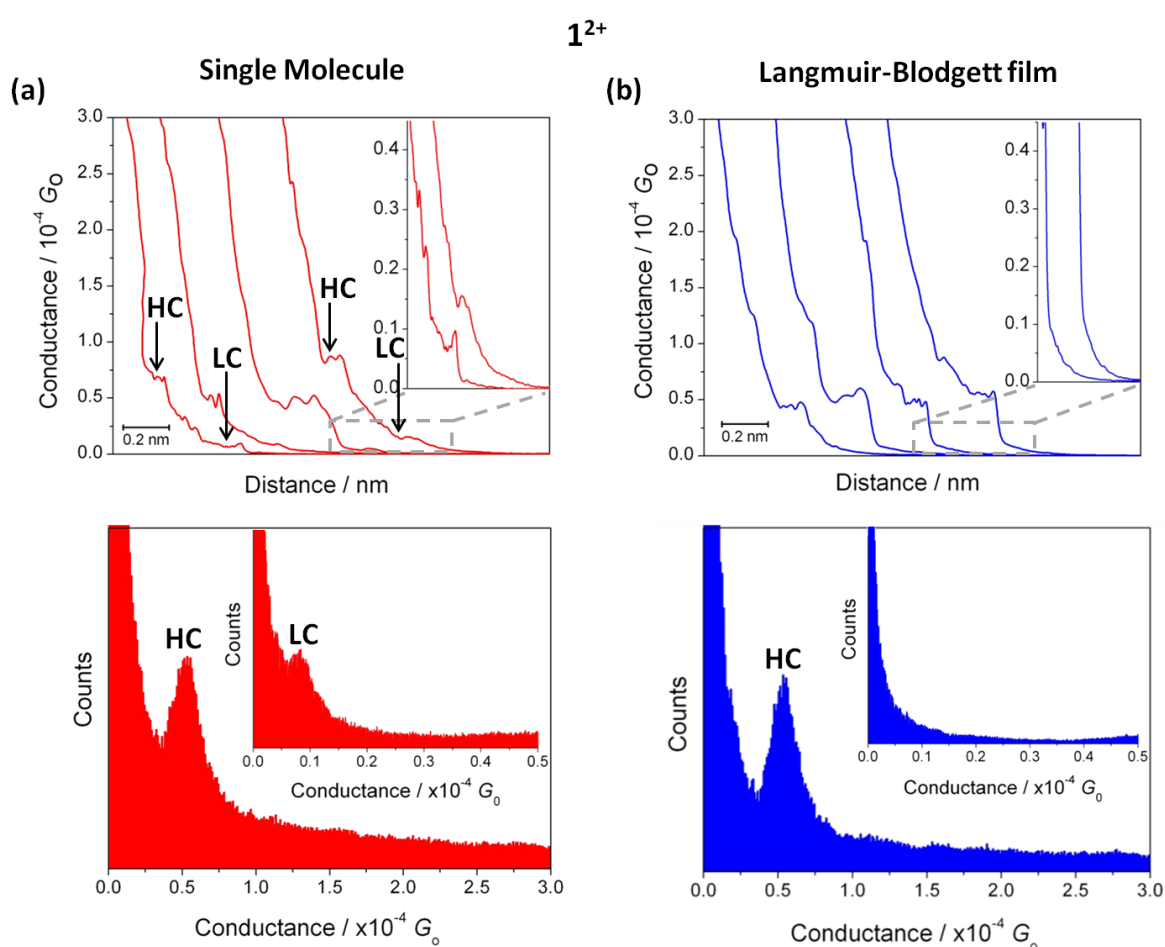
1²⁺

8

Figure 2. (a) Representative $I(s)$ traces at a set-point current of 40 nA for single molecule junctions of $\mathbf{1}^{2+}$ and conductance histogram built from summation of conductance traces (ca. 500) that show discernible plateaus. (b) Representative $I(s)$ traces for molecular junctions formed from a LB film of $\mathbf{1}^{2+}$ and conductance histogram built from summation of conductance traces (ca. 500) that shows discernible plateaus. $U_t = 0.6$ V where U_t is the "*tip bias*".
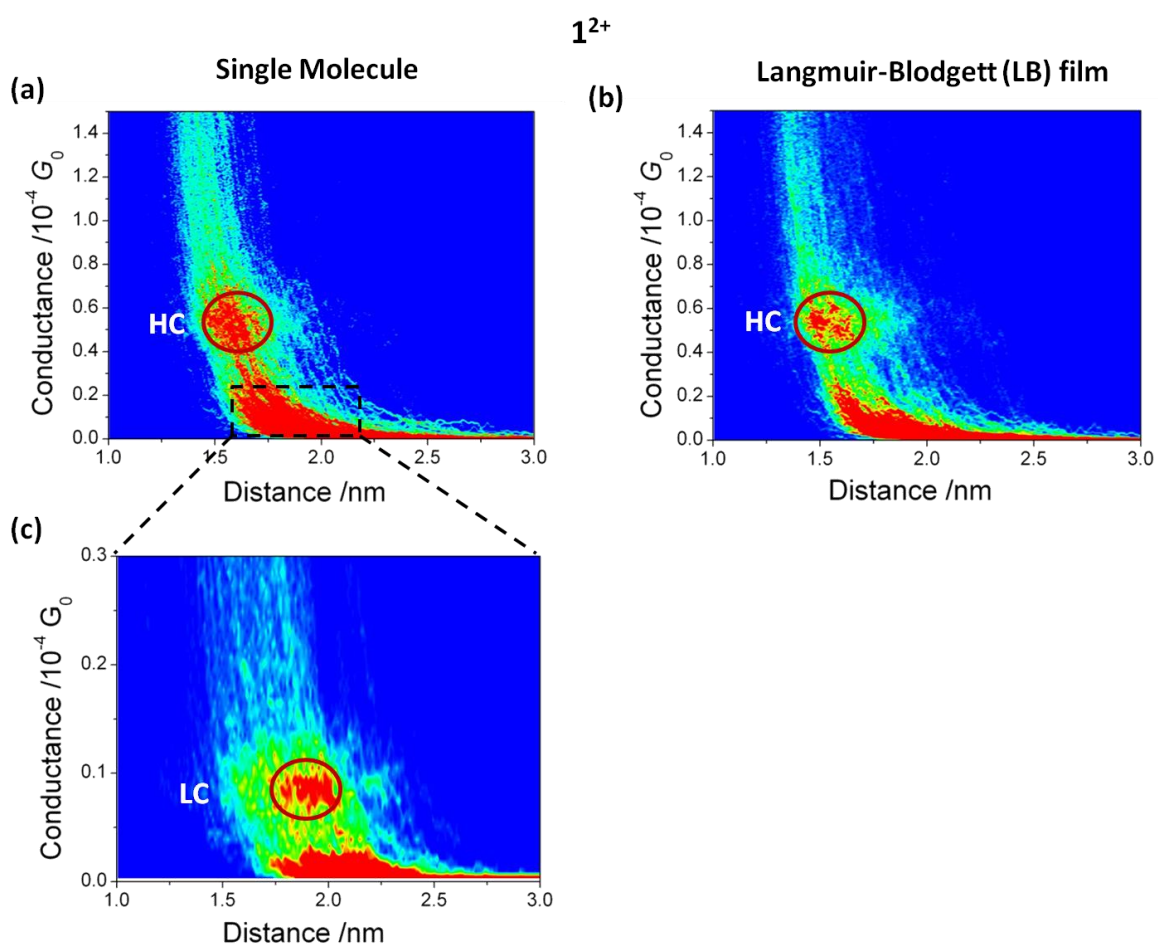

Figure 3. 2D conductance histograms for (a) a low coverage phase, single molecule, and (b) for molecular junctions formed from a LB film of [$\mathbf{1}$](BF$_4$)$_2$ (c) 2D-histogram constructed by using only the $I(s)$ curves which present the plateau corresponding to the low conductance (LC) value observed for single-molecule junctions of $\mathbf{1}^{2+}$ in Figure 2a.

The conductance value determined from this LC group is also in excellent agreement with the single molecule conductance reported for [1](BF$_4$)$_2$ in an ionic liquid (1-butyl-3-methylimidazolium triflate (BMIM-OTf)), ~0.8×10^{-5} G_0.[30] Similarly for a viologen derivative with alkyl chains as *N,N'*-substituents and using thiols as anchoring groups (*N,N'*-di-(6-(thioacetyl)hexyl)-4,4'-bipyridinium dibromide) which features a S…S distance of 2.4 nm, conductance values of ~0.75×10^{-5} G_0 and ~0.7×10^{-5} G_0 were recorded in BMIM-OTf [30] and in air,[11] respectively, with break-off distances of ~2 nm.[11] These results suggest that the LC group arises from molecular junctions in which **1**$^{2+}$ is contacted through the TMSE groups in an extended molecular geometry (Figure 4b).

The *I*(*s*) curves from molecular junctions formed from the more densely packed LB films of [1](BF$_4$)$_2$ (Figure 2b) and the conductance histogram, constructed from 500 *I*(*s*) curves, (Figure 2b bottom) also present a set of HC plateaus at $(5.4 \pm 0.95)\times10^{-5}$ G_0 with associated break-off distance of (1.56 ± 0.09) nm, Figure 3b. In contrast to junctions formed from the low surface coverage substrates featuring more isolated molecules, single-molecule junctions formed from the LB film do not show any other set of plateaus (insets in Figure 2b). The observation of a unique set of plateaus for junctions formed from LB films of [1](BF$_4$)$_2$ indicates a more uniform and less mobile molecular conformation within the junction, which is likely to be a consequence of the tight packing and high surface coverage in the film. It has been previously demonstrated that the touch-to-contact method, where an STM tip is brought into contact with a high coverage monolayer also reveals the same single molecule conductance as more established methods such as the I(s) method on dilute (low coverage) films of the same molecule.[20,43] It should be noted here that this method of measurement is likely to be locally destructive for the monolayer structure, since the initial distance between the tip and the substrate is less than the LB film thickness; in other words, the tip penetrates into monolayer.

As a consequence of tip intrusion into the monolayer, the molecule (or molecules) initially trapped within the junction must presumably tilt toward the substrate surface in order to compensate for the vertical approach of the tip. Then, during measurement, the molecule is "lifted" by the retracting STM tip, until the molecule bridge breaks.

The similarity between the high conductance, HC, values and break-off distances for the junctions formed from both single-molecule ((5.3 ± 0.85)$\times10^{-5}$ G_0; 1.60 ± 0.11 nm) and the LB film ((5.4 ± 0.95)$\times10^{-5}$ G_0; 1.56 ± 0.09 nm) indicate that $\mathbf{1^{2+}}$ is found in the same configuration in both cases. In seeking to better define the molecular geometry in the junctions, the thickness of a LB film of [$\mathbf{1}$](BF$_4$)$_2$ was determined to be (1.40 ± 0.20) nm by scratching the film with the AFM tip (see SI for more details).[43] The film thickness obtained using this method (Figure S7) is in good agreement with the break-off distances for the HC plateaus, if one considers that during junction extension only one leg of the molecule is "lifted" until the molecular bridge breaks as in Figure 4a. The film thickness and break-off distances are both considerably shorter than the Si…Si distance (2.0 nm) calculated for $\mathbf{1^{2+}}$, but entirely consistent with the configuration shown in Figure 4a in which the viologen moiety is linked to one of the electrodes and one of the TMSE end groups is in contact with the top contact electrode. The HC contact in both single-molecule and LB film junctions is therefore attributed to this conformation. A similar orientation of viologen derivatives was described previously in other LB films containing this moiety.[24, 25]
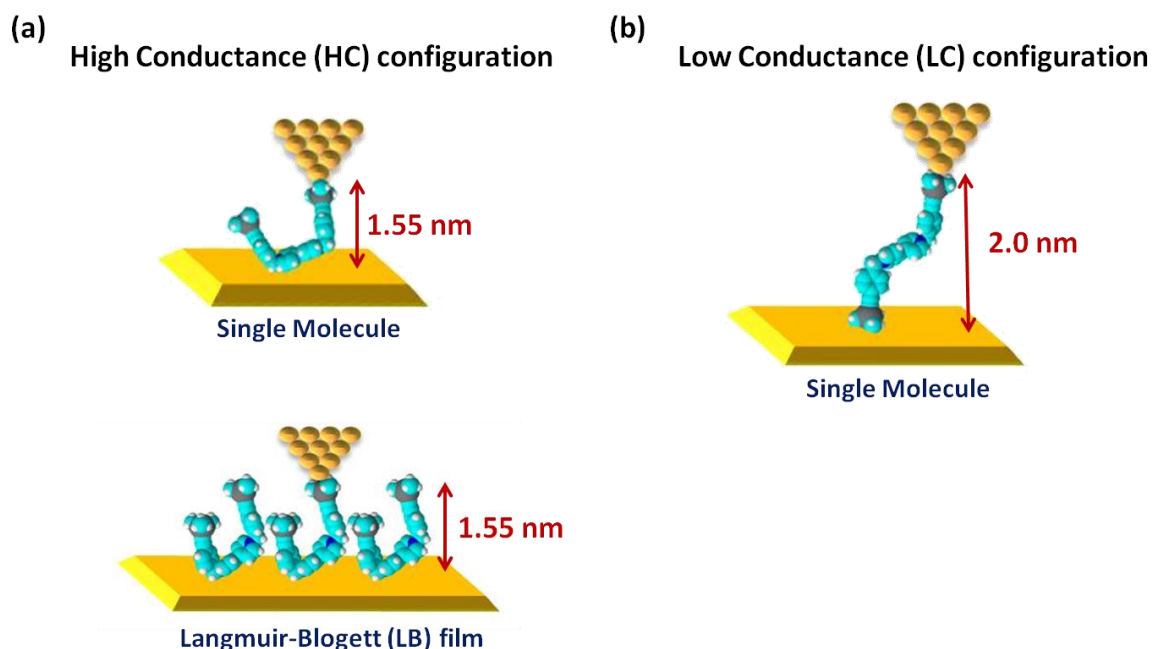

(a)
High Conductance (HC) configuration

1.55 nm

Single Molecule

1.55 nm

Langmuir-Blogett (LB) film

(b)
Low Conductance (LC) configuration

2.0 nm

Single Molecule

Figure 4. The proposed configuration of $\mathbf{1^{2+}}$ for (a) the high conductance (HC) pathway and (b) the low conductance (LC) pathway from Spartan®08V 1.0.0 molecular models.

To corroborate all these results, single-molecule conductance measurements were carried out for compound 2^{2+} (also as the bis(tetrafluoroborate) salt), which features the viologen group, but only one benzyl-supported trimethylsilylethynyl moiety (Figure 1). Figure 5a shows the 2D conductance histogram built from summation of conductance traces (ca. 500) that shown discernible plateaus as described in the Supporting Information. A conductance peak at $(5.3 \pm 0.70) \times 10^{-5}\ G_0$ and a break-off distance of (1.52 ± 0.07) nm were obtained. Both the conductance value and the break-off distance are in excellent agreement with the HC value recorded for 1^{2+} in single-molecule and LB film-based junctions, supporting the proposed configuration shown in Figure 5a as being responsible for the HC pathway.

The efficacy of the viologen contact can be appreciated by comparison with the conductance data obtained from the linearly conjugated wire-like molecule **3**, which features the TMSE surface binding groups in a similar Si...Si distance as that proposed for the HC junctions from 1^{2+}. A 2D conductance histogram constructed from data collected from single molecule junctions of 1,4-bis(trimethylsilylethynyl) benzene (**3**) under identical conditions shows a single conductance peak at $(1.25 \pm 0.50) \times 10^{-5}\ G_0$, some $4 - 5$ times lower than the viologen/TMSE contacted compounds 1^{2+} (HC) and 2^{2+}, despite the comparable break-off distance (1.41 ± 0.12) nm (Figure 5b).

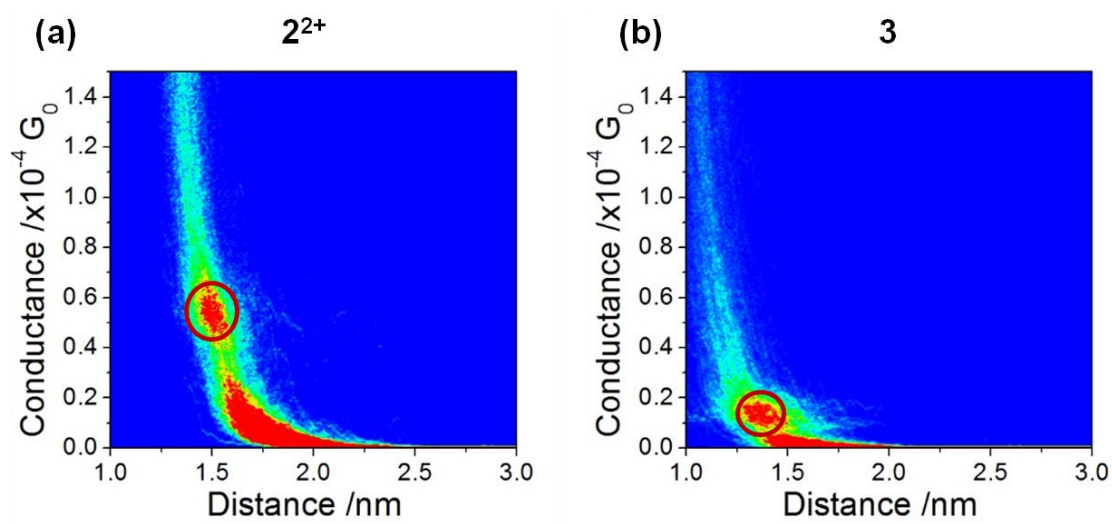**Figure 5**. 2D conductance histograms for (a) a single molecule of 2^{2+} and (b) a single molecule of **3**.

Conclusions

The electrical properties of single-molecule junctions prepared from substrates with low surface coverage of [**1**](BF_4)$_2$ ($\Gamma = 1.25 \cdot 10^{-11}$ mol·cm^{-2}) and LB films with considerably higher surface coverage ($\Gamma = 2.0 \cdot 10^{-10}$ mol·cm^{-2}) have been examined by the scanning tunneling microscope-based $I(s)$ technique. From junctions prepared from isolated molecules, two conductance values were observed. The low conductance (LC) junction has been associated to the conventional 'end-to-end' contacted molecule, with the two trimethylsilylethynyl (TMSE) groups linked to the electrodes giving rise to an extended molecular conformation within the junction. The high conductance (HC) junction has been associated with a conformation which viologen fragment contacts to one of the electrodes and a TMSE group to the other one. From junctions formed from single molecules constrained into LB films only a single high conductance (HC) junction has been observed. Therefore, surface coverage and molecular packing density can be used to control the geometry of molecules within molecular junctions, leading to a high degree of control over the resulting electrical properties.

Supporting Information

Fabrication and characterization of Langmuir and Langmuir-Blodgett (LB) films, single molecule and LB films conductance measurements, details of the tip to substrate calibration in the $I(s)$ technique, and determination of the thickness of the LB films.

Author Information

Corresponding author:

*E-mail: smartins@unizar.es (SM); paul.low@uwa.edu.au (PJL); R.J.Nichols@liverpool.ac.uk (RJN), pilarcea@unizar.es (PC)

Acknowledgements

Bibliographic References

1. Editorial, *Nat Nanotechnol*, 2013, **8**, 377.
2. D. Xiang, X. L. Wang, C. C. Jia, T. Lee and X. F. Guo, *Chem. Rev.*, 2016, **116**, 4318-4440.
3. A. J. Bergren, L. Zeer-Wanklyn, M. Semple, N. Pekas, B. Szeto and R. L. McCreery, *J. Phys-Condens. Mat.*, 2016, **28**, 094011.
4. C. C. Jia and X. F. Guo, *Chem. Soc. Rev.*, 2013, **42**, 5642-5660.
5. S. Karthauser, *J. Phys-Condens. Mat.*, 2011, **23**, 013001.
6. L. Sun, Y. A. Diaz-Fernandez, T. A. Gschneidtner, F. Westerlund, S. Lara-Avila and K. Moth-Poulsen, *Chem. Soc. Rev.*, 2014, **43**, 7378-7411.
7. E. Leary, A. La Rosa, M. T. Gonzalez, G. Rubio-Bollinger, N. Agrait and N. Martin, *Chem. Soc. Rev.*, 2015, **44**, 920-942.
8. X. D. Cui, A. Primak, X. Zarate, J. Tomfohr, O. F. Sankey, A. L. Moore, T. A. Moore, D. Gust, G. Harris and S. M. Lindsay, *Science*, 2001, **294**, 571-574.
9. R. H. M. Smit, Y. Noat, C. Untiedt, N. D. Lang, M. C. van Hemert and J. M. van Ruitenbeek, *Nature*, 2002, **419**, 906-909.
10. B. Q. Xu and N. J. J. Tao, *Science*, 2003, **301**, 1221-1223.
11. W. Haiss, H. van Zalinge, S. J. Higgins, D. Bethell, H. Hobenreich, D. J. Schiffrin and R. J. Nichols, *J. Am. Chem. Soc.*, 2003, **125**, 15294-15295.
12. W. Haiss, C. S. Wang, I. Grace, A. S. Batsanov, D. J. Schiffrin, S. J. Higgins, M. R. Bryce, C. J. Lambert and R. J. Nichols, *Nat. Mater.*, 2006, **5**, 995-1002.
13. L. Lafferentz, *Science*, 2009, **325**, 148-148.
14. G. Sedghi, V. M. Garcia-Suarez, L. J. Esdaile, H. L. Anderson, C. J. Lambert, S. Martin, D. Bethell, S. J. Higgins, M. Elliott, N. Bennett, J. E. Macdonald and R. J. Nichols, *Nat. Nanotechnol.*, 2011, **6**, 517-523.
15. S. V. Aradhya and L. Venkataraman, *Nat Nanotechnol*, 2013, **8**, 399-410.
16. M. L. Perrin, C. J. O. Verzijl, C. A. Martin, A. J. Shaikh, R. Eelkema, J. H. van Esch, J. M. van Ruitenbeek, J. M. Thijssen, H. S. J. van der Zant and D. Dulic, *Nat. Nanotechnol.*, 2013, **8**, 282-287.
17. S. Karthauser, *J. Phys-Condens. Mat.*, 2011, **23**.
18. G. Pera, S. Martin, L. M. Ballesteros, A. J. Hope, P. J. Low, R. J. Nichols and P. Cea, *Chem-Eur. J.*, 2010, **16**, 13398-13405.
19. L. M. Ballesteros, S. Martin, J. Cortes, S. Marques-Gonzalez, S. J. Higgins, R. J. Nichols, P. J. Low and P. Cea, *Chem-Eur. J.*, 2013, **19**, 5352-5363.
20. H. M. Osorio, S. Martin, M. C. Lopez, S. Marques-Gonzalez, S. J. Higgins, R. J. Nichols, P. J. Low and P. Cea, *Beilstein J. Nanotech.*, 2015, **6**, 1145-1157.
21. J. Inatomi, S. Fujii, S. Marques-Gonzalez, H. Masai, Y. Tsuji, J. Terao and M. Kiguchi, *J. Phys. Chem. C*, 2015, **119**, 19452-19457.
22. S. Y. Quek, M. Kamenetska, M. L. Steigerwald, H. J. Choi, S. G. Louie, M. S. Hybertsen, J. B. Neaton and L. Venkataraman, *Nat. Nanotechnol.*, 2009, **4**, 230-234.

23. P. Cea, C. Lafuente, J. S. Urieta, M. C. Lopez and F. M. Royo, *Langmuir*, 1998, **14**, 7306-7312.
24. S. Martin, A. Villares, M. Haro, M. C. Lopez and P. Cea, *J. Electroanal. Chem.*, 2005, **578**, 203-211.
25. P. Cea, S. Martin, A. Villares, D. Mobius and M. C. Lopez, *J. Phys. Chem. B*, 2006, **110**, 963-970.
26. D. J. Qian, C. Nakamura and J. Miyake, *Colloid Surface A*, 2000, **175**, 93-98.
27. D. J. Qian, C. Nakamura, N. Zorin and J. Miyake, *Colloid Surface A*, 2002, **198**, 663-669.
28. F. M. Raymo and R. J. Alvarado, *Chem. Rec.*, 2004, **4**, 204-218.
29. E. Leary, S. J. Higgins, H. van Zalinge, W. Haiss, R. J. Nichols, S. Nygaard, J. O. Jeppesen and J. Ulstrup, *J. Am. Chem. Soc.*, 2008, **130**, 12204-12205.
30. H. M. Osorio, S. Catarelli, P. Cea, J. B. G. Gluyas, F. Hartl, S. J. Higgins, E. Leary, P. J. Low, S. Martin, R. J. Nichols, J. Tory, J. Ulstrup, A. Vezzoli, D. C. Milan and Q. Zeng, *J. Am. Chem. Soc.*, 2015, **137**, 14319-14328.
31. S. Takahashi, Y. Kuroyama, K. Sonogashira and N. Hagihara, *Synthesis*, 1980, 627-630.
32. E. R. Janecek, U. Rauwald, J. del Barrio, M. Cziferszky and O. A. Scherman, *Macromol. Rapid Comm.*, 2013, **34**, 1547-1553.
33. R. J. Nichols, W. Haiss, S. J. Higgins, E. Leary, S. Martin and D. Bethell, *Phys. Chem. Chem. Phys.*, 2010, **12**, 2801-2815.
34. W. Haiss, D. Lackey and J. K. Sass, *J. Chem. Phys.*, 1991, **95**, 2193-2196.
35. G. Sauerbrey, *Z. Phys.*, 1959, **155**, 206-222.
36. S. Martin, I. Grace, M. R. Bryce, C. S. Wang, R. Jitchati, A. S. Batsanov, S. J. Higgins, C. J. Lambert and R. J. Nichols, *J. Am. Chem. Soc.*, 2010, **132**, 9157-9164.
37. W. Haiss, S. Martin, E. Leary, H. van Zalinge, S. J. Higgins, L. Bouffier and R. J. Nichols, *J. Phys. Chem. C*, 2009, **113**, 5823-5833.
38. G. Sedghi, L. J. Esdaile, H. L. Anderson, S. Martin, D. Bethell, S. J. Higgins and R. J. Nichols, *Adv. Mater.*, 2012, **24**, 653-657.
39. S. Sek, A. Misicka, K. Swiatek and E. Maicka, *J. Phys. Chem. B*, 2006, **110**, 19671-19677.
40. S. Sek, *J. Phys. Chem. C*, 2007, **111**, 12860-12865.
41. S. Sek, A. Tolak, A. Misicka, B. Palys and R. Bilewicz, *J. Phys. Chem. B*, 2005, **109**, 18433-18438.
42. L. M. Ballesteros, S. Martin, G. Pera, P. A. Schauer, N. J. Kay, M. C. Lopez, P. J. Low, R. J. Nichols and P. Cea, *Langmuir*, 2011, **27**, 3600-3610.
43. S. Ranganathan and R. L. McCreery, *Anal. Chem.*, 2001, **73**, 893-900.